PrinciResnet Brain Tumor Classification Technique for Multimodal Input-level Fusion Network

Padma Usha.M[a], G.Kannan[b], S. Sai Akshay[c], Giri.S[d], Shaik Mohammed Huzaifa[e]

[a&b] *Department of Electronics and Communication Engineering, B.S.Abdur Rahman Crescent Institute of Science and Technology, Vandalur, Chennai, India. padmausha@crescent.education , OrcID:https://orcid.org/0000-0002-0174-4250,kannan@crescent.education, OrcID: https://orcid.org/0000-0001-9060-1317*

[c,d,&e] *Dept. of Electronics and Communication Engineering, B.S.Abdur Rahman Crescent Institute of Science and Technology, Vandalur, Chennai, India*.

Abstract:

Brain tumors are a leading cause of mortality in India, with over 28,000 cases reported annually, resulting in more than 24,000 deaths per year, according to the International Association of Cancer Registries. Early detection, segmentation, and accurate classification are crucial in effective tumor analysis, and various algorithms have been developed to achieve this. In this study, we propose a novel approach for the detection and classification of brain tumors using both single slices of MRI and CT, as well as input-level fused images of MRI & CT. Our approach involves the implementation of the PrinciResnet brain tumor classification technique, which is based on Principal Component Analysis (PCA) and Resnet techniques. We report that our approach significantly improves the accuracy, sensitivity, and specificity parameters to 90%, 96%, and 95%, respectively, based on a dataset of 600 fused slices and 1000 single slices obtained from reputable sources. Our findings hold promise for improving the diagnosis and treatment of brain tumors, which are a significant cause of mortality globally.

Keywords: PCA, Resnet, Skip connection, Brain tumor, CT, MRI

1. INTRODUCTION

About seven brain tumors per 100,000 people are diagnosed worldwide each year, making up 2% of all tumors. The death rate is the highest for children under the age of 12 and the tenth highest for adults. Thus, a current area of medical research is localization and brain tumor segmentation [1]. Apart from accurate localization, segmentation, and brain tumor classification, the reduction of redundant pixels is considered an important part of image processing which in turn improves the efficiency of the process[2]. That is energy compaction and decorrelation are two eyes of preprocessed images after which processing is made easier. Various techniques are existing for obtaining decorrelated images. One of the best methods which is a statistical method in image processing to make the image more energy compacted and decorrelated is Principal component analysis(PCA). This method is based on obtaining Eigen values and Eigen vectors of an image. Then this preprocessed image is given to the deep learning architecture Resnet which is a deep learning algorithm which is an architecture introduced by Microsoft research in 2015 to overcome the vanishing gradient problem. This architecture uses residual blocks to overcome the vanishing gradient/exploding problem. It is challenging to learn and adjust the parameters of the network's early layers due to the vanishing gradient problem. In contrast, when the backpropagation algorithm advances causing gradient descent to diverge. This is called an exploding gradient problem. The residual block in Resnet has skip connections which overcome the vanishing gradient problem.

Paper 16 compares various PCA algorithms on MRI images followed by the application of the clustering algorithm. The hybrid attention block improves the characteristics that each encoder individually obtains from the respective imaging modality's low-level features. The decoder restores the results of the pixel-level segmentation after combining with the high-level semantic of the decoder path through skip convolution[1]. PCA and Superpixels are used to extract key features that enable the precise detection of brain malignancies. It increases data interpretability with minimal data loss[2]. Data imbalance has long been a problem in brain tumor segmentation.

Researchers test various approaches, including multi-task learning, network cascade and ensemble, and specialized loss functions, to solve the imbalance problem. Making the most of multi-information modalities is another option. Modality fusion and addressing the modality missing have been the subject of recent research[3]. Accuracy rates rise when feature vectors are restricted to the PCA's preferred component[4]. It is vital to provide the diagnostic system with all the information that is present in the tumor region to develop a powerful diagnostic system that will appropriately classify brain tumors[5].

Skip connections are well utilized for Unet architecture to increase its efficiency[6]. The promise for machine learning and deep learning approaches to improve medical image analysis for disease diagnosis and detection, but also the necessity for collaboration among physicians, researchers, and data scientists to address the problems involved with medical image analysis[7]. Machine learning has the potential to improve the accuracy of medical picture classification, which could have important consequences for breast cancer detection and therapy[8]. PCANet, which extracts features from photos using a two-stage convolutional neural network (CNN). The authors show how PCANet works on different benchmark datasets and highlight its potential for practical applications in computer vision and image analysis[9]. PCA's efficiency in decreasing the computational complexity of image processing jobs while keeping the image's significant visual qualities. This can significantly increase the efficiency of image analysis and related applications[10]. PCA has been used in medical image processing for dimensionality reduction, noise reduction, and picture segmentation. According to the findings, PCA could be a beneficial method for increasing the accuracy and efficiency of medical image analysis and associated applications[11]. The findings show that the suggested method could have important implications for accurate and efficient brain tumor diagnosis utilizing medical imaging[12].

The contribution of our work is

1. Dimensionality reduction of input images and given as input to deep learning algorithm (Resnet architecture).
2. ResNet enhances the performance of deep neural networks by adding more neural layers while reducing error percentage.
3. This reduces the execution time of the algorithm.

This paper is organized as follows: Initially, the introduction section provides the current scenario of the proposed problem and research gap. Also, this section discusses existing methods and conveys the proposed method to fill the research gap. The next section is materials and methods which describes the detailed explanation of the data implemented for this research. A Detailed explanation of the proposed method. Results and discussions are in the next section.

2. Materials and Methods

The PrinciResnet method consists of the following sequences: Pre-processing, dimensionality reduction, and classification using the Resnet technique. This method was implemented in MATLAB 2019a version. Multimodal images such as MRI and CT were considered for analysis[6].

2.1 Preprocessing

The same slices of MRI and CT were downloaded from http:// www.med.harvard.edu/AANLIB/home.html of resolution 256X256 with file format in Graphics interchange file(gif) which is then resized to Spatial resolution 224X224X3 and file format has been changed to Joint Photographic Experts Group (jpeg) whereas different slices of MRI and CT were downloaded from www.kaggle.com[14]. In this, MR T1, T2, MR Gadolinium, and Proton density slices were considered for MRI images. Patients affected with Glioma, Sarcoma, and Meningioma are downloaded from the Medharvard website[15]. Around 100 MRI images and 100 CT images of the same slices are considered. This accounts for individual slices of 200 images[16]. Also, around 100 images of CT and MRI were downloaded from www.kaggle.com which are with different slices.

2.2 Methodology

2.2.1 Principal Component Analysis (PCA)

Principal Component Analysis (PCA) is a commonly used method for reducing dimensionality, and it is particularly effective for transforming data from a higher-dimensional space to a lower-dimensional space [5]. Eigenvectors are found in PCA which gives the direction of pixels having a higher variance. An image is decomposed into various of its components in which the principal component has energy compact and decorrelated features with a high reduction in its dimensions[17]. This principal component can be used for further analysis in the whole image processing sequence. The Process of principal component analysis is as follows,

- Find the covariance matrix which is given by,

$$C = \frac{1}{n} \sum_{a=1}^{n} \left(P_a - \overline{P}\right) . \left(P_a - \overline{P}\right)^T \quad (1)$$

$\left(P_a - \overline{P}\right)$ → Shape distortion

- $C = D \Lambda D^T$, D=[s_1,s_2----------s_{2n}] (2)

The above 2n x 2n unitary matrix of eigenvectors s_k of C and Λ is the diagonal matrix of eigenvalues λ_1, λ_2, λ_3 ---------- which sums up to λ_k.

- The new axes s_k in feature space leads to various directions of variation that are mutually not correlated.
  $\sqrt{\lambda_k}$ is the standard deviation along s_k of all the structures
- An image model can then be represented in terms of PCA as,

$$P = \overline{P} + \sum_{k}^{2n} c_k \, s_k \, , \quad (3)$$

c_k → coefficients

- Every eigenvector s_k has a corresponding eigenvalue λ_k, and $\lambda_1 \geq \lambda_2 \geq \lambda_3$----------, variability is defined by the principal mode of variation. Hence, due to this number of degrees of freedom is consistently decreased.[18]

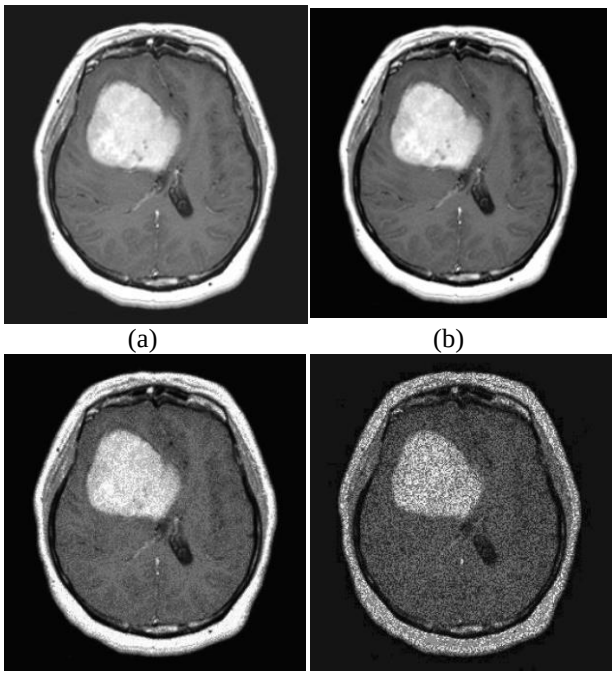

(a) (b)

(c) (d)

Fig 1. The input image is shown in Fig (a), and three components of the input image are shown in Figures (b), (c), and (d) in which the principal component(PC) has distinct features.

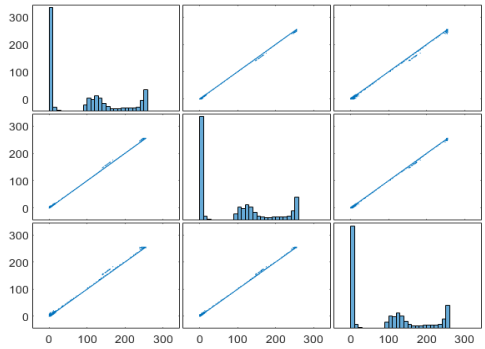

Fig 2. Plot matrix for input image with redundancy

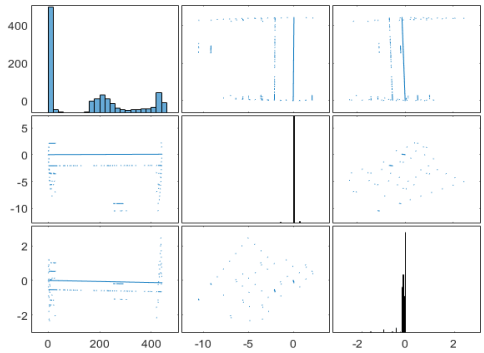

Fig 3. Plot Matrix for PC1 without redundancy

In Fig.1, the three components of input images were shown. The principal component is given as input to the deep learning algorithm which is Resnet34 architecture. By implementing PCA in the input image the significant amount of dimensions has been reduced[19]. In our work, principal component analysis (PCA) was effectively used to produce principal components. Pairplots were plotted as in Fig.2 and Fig.3 to compare the pairwise correlations in the original data with those in the main components to judge how well the PCA reduced redundancy and achieved data reduction. We saw that the main components completely removed the connection between the variables contained in the original data, showing a considerable decrease in correlation. Furthermore, the diagonal distribution plots showed that the PCA successfully transferred compressibility-related variance. Our research suggests that the PCA was successful in data compression and redundancy reduction overall.

In Fig.4 of the proposed model block diagram, an input image consisting of separate slices of MRI or CT or fused slices of MRI & CT [20] is given as input to the proposed model. Preprocessed image is obtained by resizing the image and data augmentation [21] is also performed to increase the number of input image slices. Then, dimensionality reduction of the preprocessed image is obtained by making use of the PCA method in which the principal component is given as input to the Resnet34 model[22]. Finally, classification is done by using the Resnet34 model. The advantages of both PCA which is dimensionality reduction and the Resnet34 model which is to overcome the vanishing gradient problem/exploding problem are combined in this model which increases the accuracy in determining the tumor or non-tumor problem[23].

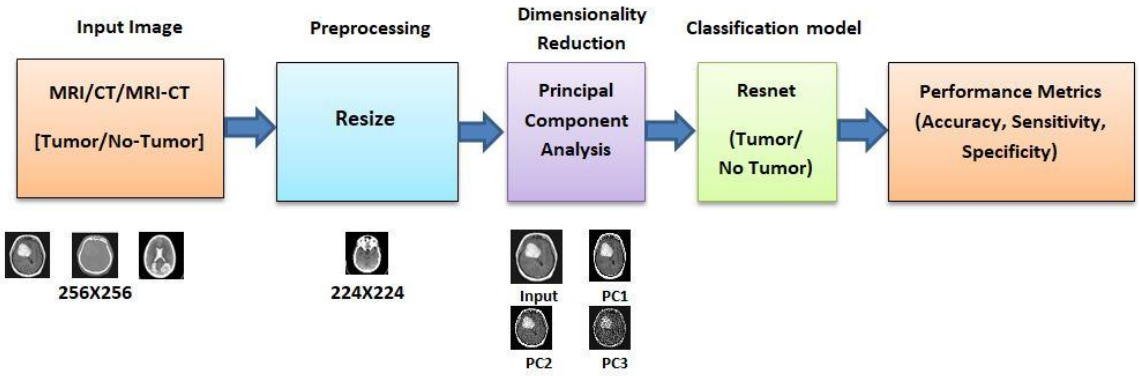

Fig 4. Block diagram of the PrinciResnet model

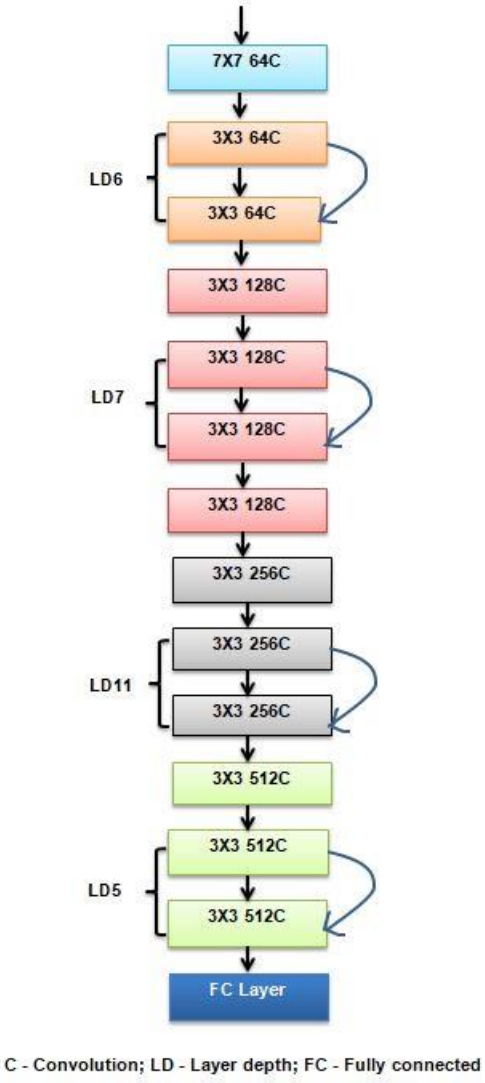

Fig 5. Resnet layered architecture

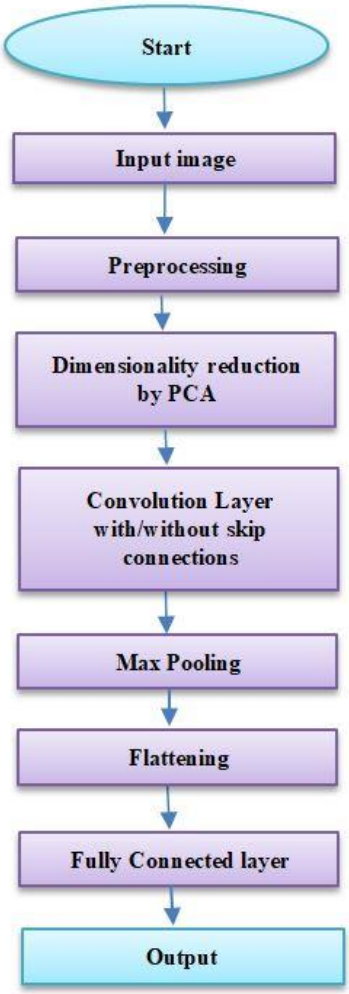

Fig 6. Flow diagram of the PrinciResnet model

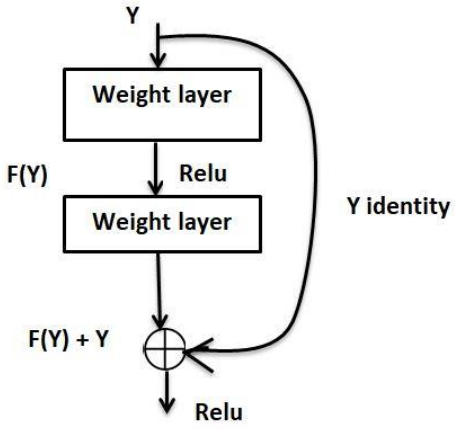

Fig 7. Skip connection of Resnet architecture

2.2.2 Deep learning model- Resnet34

In the Resnet34 model, the principal component image of size 224X224 is given as input to the Resnet34 model. This is convoluted with the kernel size 7X7, 64 filters followed by resizing of the output feature map with maximum pooling layer. Then again convolution is performed with a 3X3 filter size with 64 filters having a layer depth of 6 after which is forwarded to the next layer which has again kernel size of 3X3 with 128 filters of layer depth of 7. Then it is forwarded to the layer which has a filter size of 3X3 with 256 filters of layer depth as 11. Then this passed to the next layer of kernel size as 3X3 of 512 filters with a layer depth of 5X5. Then this is resized using the average pooling layer. Among all the layers, Resnet34 consists of only two pooling layers, and all other layers belong to the convolution layer[24]. Here, to overcome the problem of vanishing gradient and exploding problem, skip connections are introduced in between the layers in which input from specific layers are skipped to pass on through the next layer and instead it passes on to two layers ahead. This is the way the limitation of Resnet has been overcome. The figure depicts the simplified network design of the Resnet34 model and its skip connection. At last, the neural network takes the output column vector as an input to classify it as a tumor or non-tumor image.

Each one of the convolution operations also acts in the form of a residual function, adding the input to the block element by element to the convolutional operation's non-linear output feature maps which is shown in Fig 5. Utilizing these skip connections speeds up convergence[5]. This addresses the degradation issue that arises with such deep networks[5]. The flow diagram Fig.6 shows the process steps of the proposed PrinciResnet algorithm. The process is as follows, first preprocessing is initiated for the resizing of images, then Principal component analysis (PCA) is applied for the drastic decrease in dimensionality which is followed by CNN Resnet architecture with a skip connection. This comprises the convolution layer, ReLU layer, and pooling layer. Here, the skip connection is introduced in Fig.7. This is followed by a flattening layer, then a fully connected layer which is used to pass the signal to the neuron cells for tumor detection. Then the output is displayed as tumor detected or not.

3. Results and Discussion

Initially, the PCA method is implemented input image to reduce the dimension of the same. Then, the input image is passed onto the Resnet34 model which is built with 34 convolutional layers, and 16 skip connections to avoid the vanishing gradient problem. Layer block includes conventional convolution neural network block along with skip connection which is called a single residual block. In this results and discussion section figures shown corresponds to the connection of single residual block layers along with a single skip connection. This single block is repeated 16 times to get the Resnet34 model. In a single residual block, the input image is connected to convolution layer 1, then batch normalization 1, then to Rectified linear unit1 (ReLU1) in which the right branch is connected to maximum pooling layer1 next to which it is connected to convolution layer 2, then batch normalization 2, then ReLU2, which it is connected to convolution layer 3, batch normalization 3 and the left branch is connected to skip convolution. The addition layer at the bottom has two inputs one is from skip convolution and the other is from batch normalization and then the added layer output is given to the ReLU3 layer. All these connections comprise a single residual block. By giving the skip connection process, the vanishing gradient problem doesn’t occur in the architecture.

Also training report has been generated for a

single residual block for the maximum epoch of 5 and then it is tried for the maximum epoch of 50. This is depicted in Figs 10 & 11. A minimum number of epochs gives a training accuracy of less than 50% and when it reaches it provides maximum accuracy of 92%. It is revealed exactly that whenever epochs are increased accuracy also is increased. Coming to the loss parameter when the number of epochs is 5 this parameter attained a maximum value of 80% and when the epoch number is increased loss parameter reached almost zero.

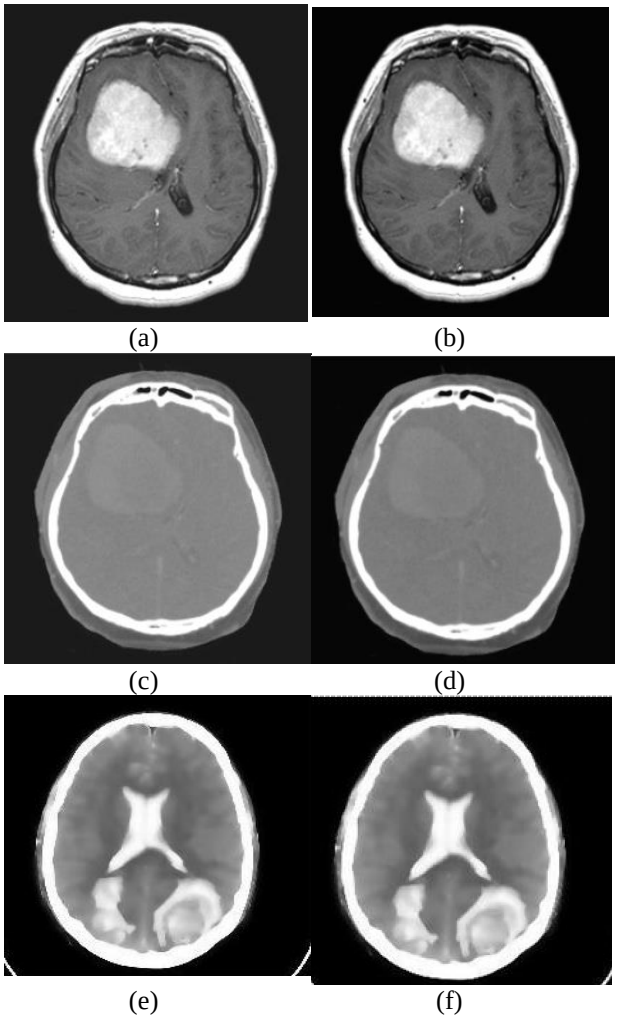

Fig 8. Input images (a) MRI brain tumor image (c) CT brain tumor image (e) Fused (MRI & CT) brain tumor image Principal component of (b) MRI brain tumor image (d) CT brain tumor image (f) Fused (MRI & CT) brain tumor image

Fig 8 shows the possible combination of input images. This proposed method combines the methods of PCA and Resnet34 and it categorizes tumor or no-tumor for three different modalities, one is MRI, another one is CT and the last one is a combined version of the modalities such as MRI with CT fused. Thus, the PrinciResnet method resolves the problem of inaccurate detection of tumors, and tumor classification can be made before the treatment and after the treatment since usually, MRI-CT images will be fused once the patient has undergone surgery and has to be detected residual tumor cells after post-operation[25]. Fig 9 shows the creation of layers and their connections in the MATLAB simulation environment. In this process, every conventional layer has been added and then a skip connection has to be added at the appropriate layer which is vital in Resnet architecture.

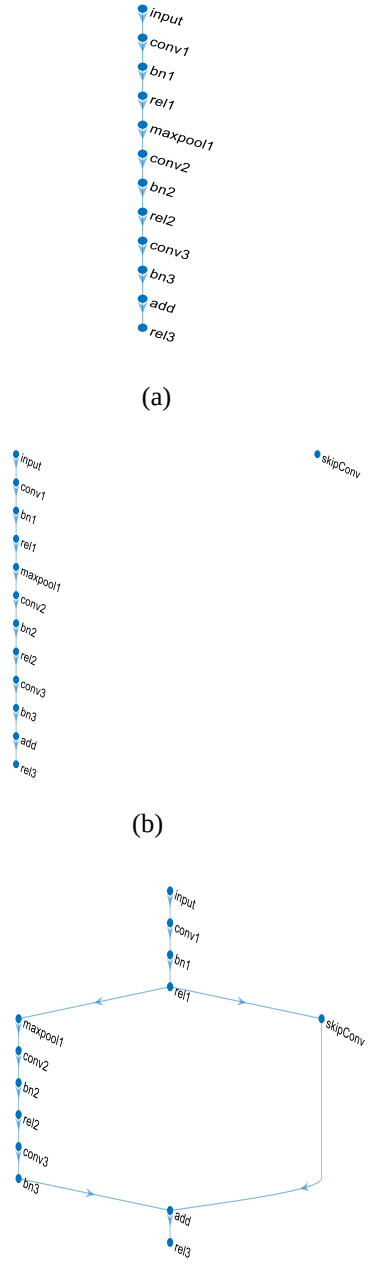

Fig 9 (a) to (c) represents the addition of Standard Residual block with skip convolution in the simulation environment continuously.

Table 1. Tumor classification label and its count in the training phase

Label	Count
CT_No Tumor	16
CT_Tumor	8
MRI_No Tumor	17
MRI_Tumor	11
MRI-CT_No Tumor	2
MRI-CT_Tumor	3

Table 1 shows the classification labels and their count in the training phase. For the single residual block, the confusion matrix shown in Fig 10 has been plotted which it categorizes into 6 different types. Diagonal values represent true positives for all six categories of classification. CT with no tumor, CT with tumor, MRI with no tumor, MRI with tumor, MRI-CT fused image with no tumor, and at last MRI-CT with tumor.

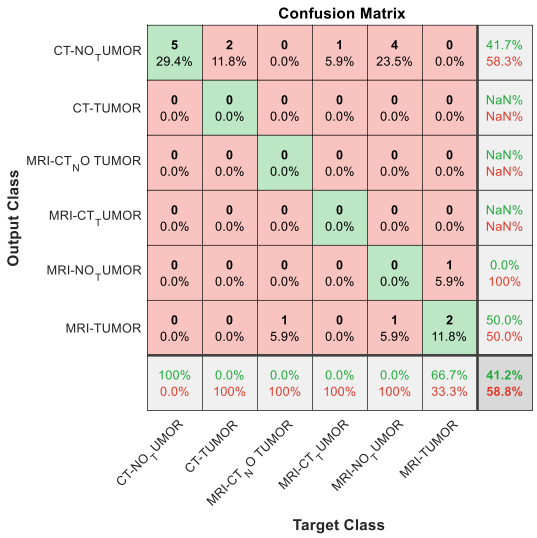

Fig 10. Confusion matrix for a given set of images for a single residual block

Fig 11. Training Progress showing Accuracy and Loss for a single residual block for the epoch of 5

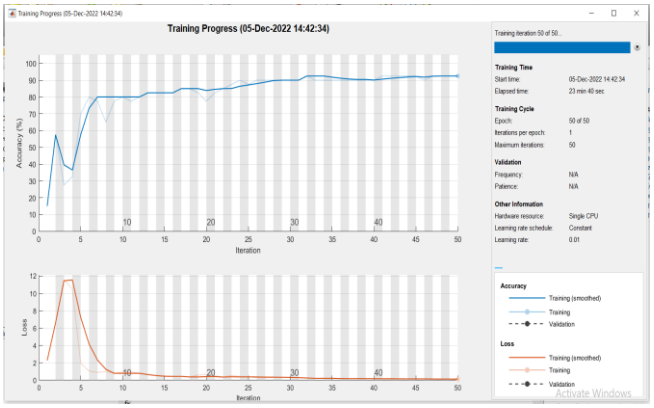

Fig 12. Training Progress showing Accuracy and Loss for a single residual block for the epoch of 50

Figure 6 and 7 shows the accuracy and loss for the 5th epoch and 50th epoch considered for analysis. It demonstrates that as the epoch number grows, so does accuracy and loss function decreases.

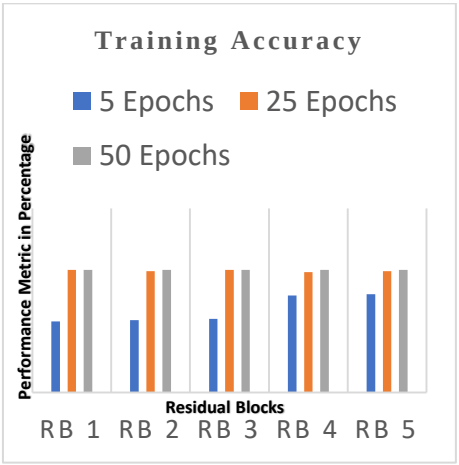

(a)

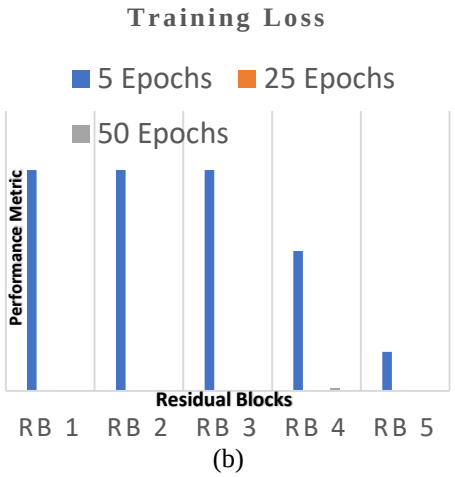

(b)

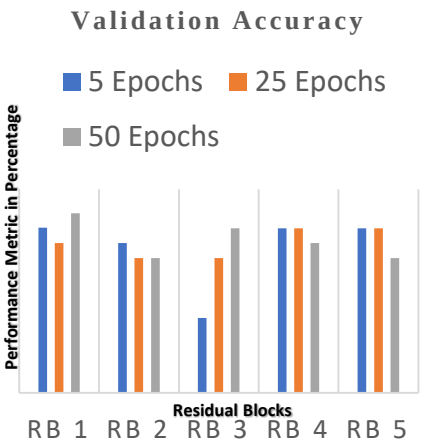

(c)

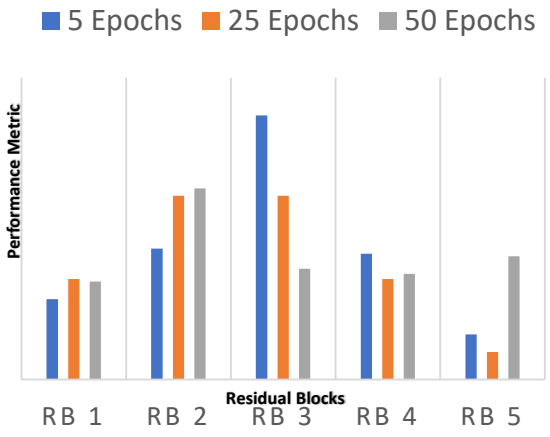

(d)

Fig 12. Graphs (a) to (d) represent training accuracy and loss, validation accuracy and loss from 1st Residual Block to the 5th Residual Blocks for 5, 25, and 50 epochs.

The study examined the performance of the network model from single epoch to multiple epochs such as 5, 25, and 50, it is clear from Figure 12 represents training accuracy touches the peak point at the 50th epoch for Resnet blocks from one to five whereas validation accuracy has its peak point for single residual block. Additionally, training loss is almost zero for the 50th epoch for the fifth residual block, and validation loss is minimum at the 25th epoch of the fifth residual block. From this analysis, it is inferred that as residual block and epoch number increases desirable performance is achieved for the model.

The analysis can be further extended to a comparison of the same performance metrics as indicated above with epoch numbers varying from 5 to 50 epochs whereas earlier analysis has been chosen only for selective epochs such as 5,25 and 50 which indicates the lowest, moderate, and highest epoch. Figure 13 represents the line plots for comparison of performance metrics. As understood from the previous analysis, in this also residual block 5 at the 50th epoch outperforms other resnet blocks and epochs.

Overall, this analysis demonstrates the effectiveness of the ResNet architecture in improving the accuracy and reducing the loss in deep learning models. It also highlights the importance of choosing the appropriate number of residual blocks to achieve the best performance.

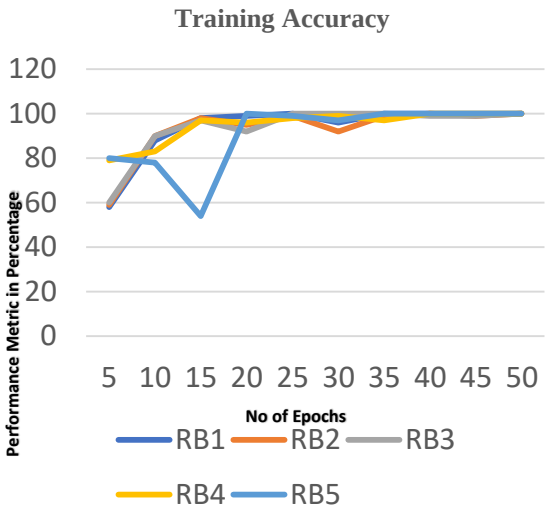

(e)

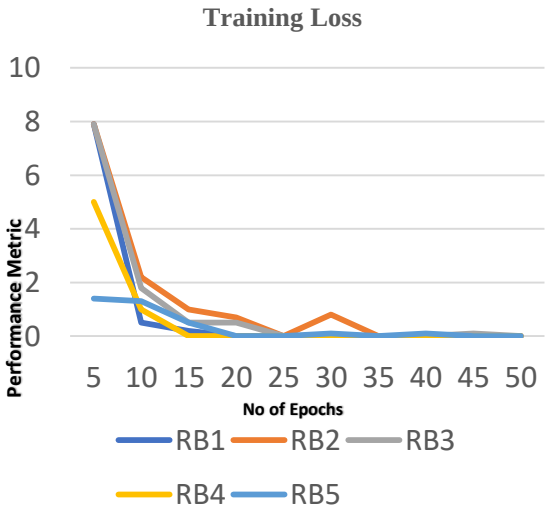

(f)

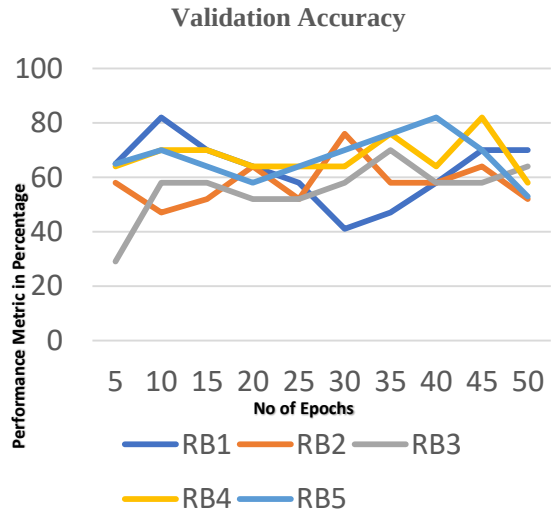

(g)

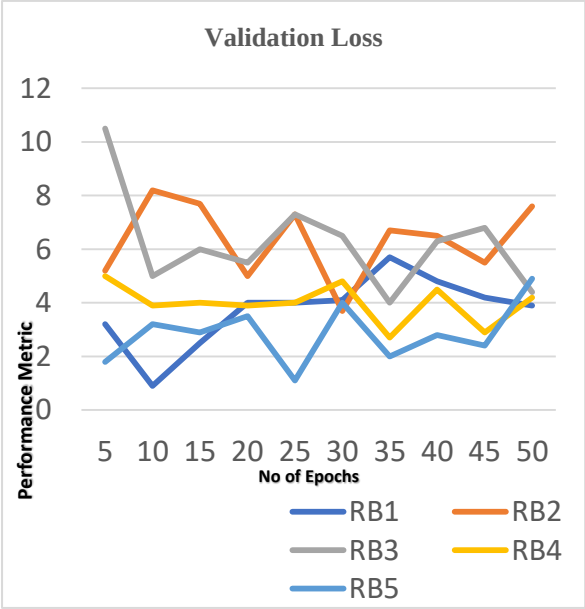

(h)

Figure 13. Graphs (e) to (h) represent line plots for training accuracy, training loss, validation accuracy, and validation loss from the 1st residual block to the 5th residual block for 5, 25, and 50 epochs.

Training Accuracy gradually increases from the first to the fifth residual block. When simulated from 5 to 50 epochs, these five residual blocks exhibit higher training accuracy than validation accuracy. Training loss appears to be less than validation loss and, in some cases, zero. Regardless of residual blocks, the parameters appear to be unpromising from 5 to 25 epochs, but promising from 30 to 50 epochs. We acquire the lowest validation loss and highest validation accuracy in the 5th Residual Block.

Table 3. 16X1 layers of a single residual block

Layer number	**Layer name**	**Layer expansion**	**Layer Description**
1	'input'	Image Input	224x224x1 images with 'zero centers' normalization
2	'conv 1'	Convolution	64 7x7x1 convolutions with stride [1 1] and padding option as 'same'
3	'bn1'	Batch Normalization	Normalization in batches of 64 channels
4	'rel1'	ReLU	Rectified Unit
5	'max pool1'	Max Pooling	Pooling 2x2 with stride [2 2] and padding [0 0 0 0]
6	'conv 2'	Convolution	64 3x3x64 convolutions with stride [1 1] and 'same' padding
7	'bn2'	Batch Normalization	Normalization in batches of 64 channels
8	'rel2'	ReLU	ReLU
9	'conv 3'	Convolution	64 3x3x64 convolutions with stride [1 1] and padding 'same'
10	'bn3'	Batch Normalization	Batch Normalization
11	'add'	Addition	Element-wise addition of 2 inputs
12	'rel3'	ReLU	ReLU
13	'FC'	Fully Connected	6 inter-connected layer
14	'soft max'	Softmax	Softmax function
15	'class output '	Classification Output	crossentropyex with 'CT-NO_TUMOR'

			and 5 other classes
16	'skip Conv'	Convolution	64 1x1x64 convolutions with stride [2 2] and padding [0 0 0 0]

Table 3 provides information about the number of layers in detail for the single residual block. The layer analysis provided describes the architecture of a neural network for image classification, with a total of 16 layers for a single residual block. It conveys layer name, layer description, and size of the input image as well as filter kernel size are indicated. This resnet block layer gets repeated till the fifth residual block.

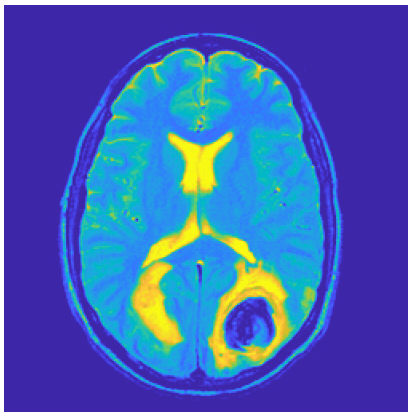

(a) Input image

(b) Convolution Layer1 activation feature maps

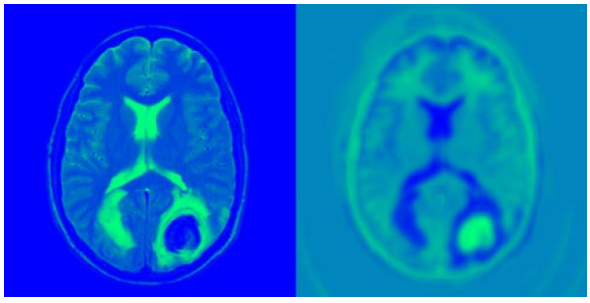

(c) Strongest activation channel of convolution layer 1

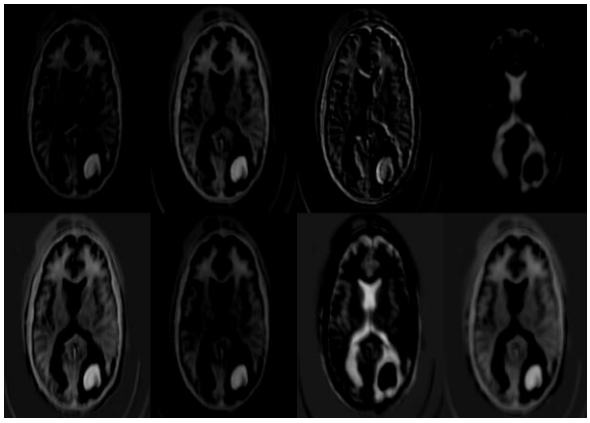

(d) Activation feature maps of ReLU layer 1

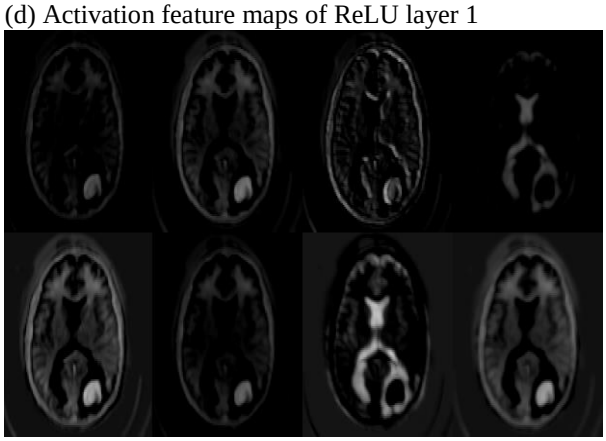

(e) Activation feature maps of Pooling Layer 1

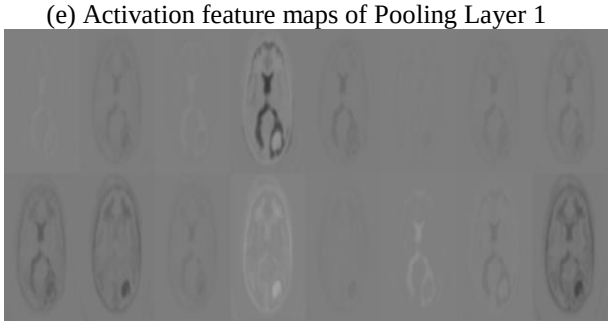

(f) Activation feature maps of convolution layer 2

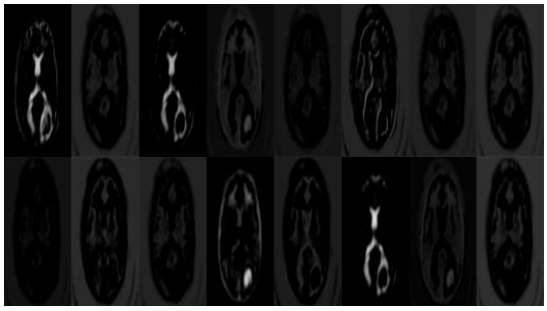

(g) Activation feature maps of ReLU layer 2

Fig 14. Activation function feature maps of various layers

Images shown above in Fig. 14 denote the activation images output of convolution layer 1,

ReLU layer 1, Pooling layer 1, convolution layer 2, and ReLU layer 2 in which convolution layer 1 extracts features like lines, edges, points, etc., ReLU layer 1 converts all negative values to zero. Pooling layer 1 downsamples the pixels in the ratio of 4:1 which acts as a dimensionality reduction tool. Various filters are used in the pooling layer to extract features of brain tumors. Activation image of convolution layer 2 extracts more features than the activation image of convolution layer 1.ReLU layer extracts more features in-depth than the convolution layer which is clearly shown in the feature map corresponding to ReLU layer 1. The pooling layer 1 activation image displays the tumor outline more clearly than ReLU layer 1. Above all, among various feature maps extracted in convolution layer 1 the strongest channel of convolution layer 1 shows the feature map in which more features are extracted among various filters of convolution layer 1 itself. As the deepness increases like 1,2,3 etc., depth in the extraction of features also increases. A single batch of layers before skip connection consists of a convolution layer, ReLU layer, pooling layer, and batch normalization. Skip connection increases the possibility of convergence than a single batch of layers handled without skip connection.

3.1 Performance metrics for validating the proposed algorithm:

An algorithm's efficiency is estimated by finding out various performance metrics. For the proposed algorithm, performance metrics such as accuracy followed by sensitivity, and specificity are calculated. The definitions of the calculated metrics are given below,

- Accuracy

  It is given by the number of accurate valuations to the number of all valuation

$$Accuracy = \frac{Number\ of\ accurate\ valuation}{Number\ of\ all\ valuation} \quad (4)$$

- Sensitivity

  It is given by the true positive count to the count of all positive valuation

$$\text{Sensitivity} = \frac{\text{Number of true positive valuations}}{\text{Number of all positive valuations}} \quad (5)$$

- Specificity

  It is given by the number of true negative valuations to the number of all negative valuation

$$\text{Sensitivity} = \frac{\text{Number of true negative valuations}}{\text{Number of all negative valuations}} \quad (6)$$

Table 4. Comparison between different classification algorithms with PrinciResnet

Reference	Method Implemented for brain tumor classification	Performance metrics
Proposed	PrinciResnet	Accuracy - 98% Sensitivity- 95% Specificity- 95%
[1]	DWT + PCA + ANN	Accuracy - 97% Sensitivity- 95% Specificity- 94%
[20]	LeaSE-DARTS	Accuracy - 91% Specificity- 98%
[15]	Data augmentation method- Cheng	Sensitivity- 91%
[21]	EADL-BTMIC Model	Accuracy - 98% Specificity- 99%

The comparison table in Table 4 compares the proposed PrinciResnet method with other classification algorithms which are constructed on Principal Component Analysis, Discrete Wavelet Transform Learning search expansion, Data augmentation method, and deep learning method[28]. It is inferred that our proposed method performs more or equal to other existing algorithms.

4. Conclusion and future work

A medical decision-making system has been developed to classify brain images affected by tumors or not by combining the Principal component analysis (PCA) dimension reduction features along with Resnet34 architecture for classification (PrinciResnet). For analysis of this algorithm, 600 slices of fused images of MRI and CT images were taken and 1000 slices of separate slices of MRI and CT images were taken. Classification accuracy and other performance metrics for this proposed method have given favorable results when compared with other similar kind of methods.

Dimensionality reduction and skip connection are the double-highlighted features of this algorithm. The uniqueness of the principle component basis is the single spatial axis is the initial main component. When each observation is projected along that axis, the resultant values form a new variable with the highest variance of any feasible first-axis possibility. As a result, the PCA was able to drastically minimize correlation. According to the distribution plots along the diagonal, PCA was similarly successful in transferring variance related to compressibility. Thus, this method can be extended

for the various brain tumor categories also. Here, we have implemented Resnet34 layers and this can be modified according to the network requirement and network performance. The outcome of this technique is to assist physicians in their diagnosis accurately. In the future, this can be further extended to segment the tumor size and extract its area. Depending on the tumor size, the tumor stage can be determined. Thus, this method is proved to be an automated efficient brain tumor classification method.

References:

[1] L. Zhao, J. Ma, Y. Shao, C. Jia, J. Zhao, and H. Yuan, "MM-UNet: A multimodality brain tumor segmentation network in MRI images," *Front. Oncol.*, vol. 12, p. 950706, Aug. 2022, doi: 10.3389/fonc.2022.950706.

[2] H. Tang and Z. Hu, "Research on Medical Image Classification Based on Machine Learning," *IEEE Access*, vol. 8, pp. 93145–93154, 2020, doi: 10.1109/ACCESS.2020.2993887.

[3] M. K. Islam, M. S. Ali, M. S. Miah, M. M. Rahman, M. S. Alam, and M. A. Hossain, "Brain tumor detection in MR image using superpixels, principal component analysis and template based K-means clustering algorithm," *Mach. Learn. Appl.*, vol. 5, p. 100044, Sep. 2021, doi: 10.1016/j.mlwa.2021.100044.

[4] Z. Liu *et al.*, "Deep learning based brain tumor segmentation: a survey," *Complex Intell. Syst.*, Jul. 2022, doi: 10.1007/s40747-022-00815-5.

[5] E.-S. A. El-Dahshan, T. Hosny, and A.-B. M. Salem, "Hybrid intelligent techniques for MRI brain images classification," *Digit. Signal Process.*, vol. 20, no. 2, pp. 433–441, Mar. 2010, doi: 10.1016/j.dsp.2009.07.002.

[6] Megha. P. Arakeri and G. R. M. Reddy, "Computer-aided diagnosis system for tissue characterization of a brain tumor on magnetic resonance images," *Signal Image Video Process.*, vol. 9, no. 2, pp. 409–425, Feb. 2015, doi: 10.1007/s11760-013-0456-z.

[7] M. Rana and M. Bhushan, "Machine learning and deep learning approach for medical image analysis: diagnosis to detection," *Multimed. Tools Appl.*, Dec. 2022, doi: 10.1007/s11042-022-14305-w.

[8] H. Tang and Z. Hu, "Research on Medical Image Classification Based on Machine Learning," *IEEE Access*, vol. 8, pp. 93145–93154, 2020, doi: 10.1109/ACCESS.2020.2993887.

[9] T.-H. Chan, K. Jia, S. Gao, J. Lu, Z. Zeng, and Y. Ma, "PCANet: A Simple Deep Learning Baseline for Image Classification?," 2014, doi: 10.48550/ARXIV.1404.3606.

[10] S. C. Ng, "Principal component analysis to reduce dimension on the digital image," *Procedia Comput. Sci.*, vol. 111, pp. 113–119, 2017, doi: 10.1016/j.procs.2017.06.017.

[11] D. Nandi, A. S. Ashour, S. Samanta, S. Chakraborty, M. A. M. Salem, and N. Dey, "Principal component analysis in medical image processing: a study," *Int. J. Image Min.*, vol. 1, no. 1, p. 65, 2015, doi: 10.1504/IJIM.2015.070024.

[12] S. B. Gaikwad and M. S. Joshi, "Brain Tumor Classification using Principal Component Analysis and Probabilistic Neural Network," *Int. J. Comput. Appl.*, vol. 120, no. 3, pp. 5–9, Jun. 2015, doi: 10.5120/21205-3885.

[13] A. Saha, Y.-D. Zhang, and S. C. Satapathy, "Brain Tumour Segmentation with a Muti-Pathway ResNet Based UNet," *J. Grid Comput.*, vol. 19, no. 4, p. 43, Dec. 2021, doi: 10.1007/s10723-021-09590-y.

[14] T. Zhou, S. Ruan, and S. Canu, "A review: Deep learning for medical image segmentation using multi-modality fusion," *Array*, vol. 3–4, p. 100004, Sep. 2019, doi: 10.1016/j.array.2019.100004.

[15] K. A. van Garderen *et al.*, "EASE: Clinical Implementation of Automated Tumor Segmentation and Volume Quantification for Adult Low-Grade Glioma," *Front. Med.*, vol. 8, p. 738425, Oct. 2021, doi: 10.3389/fmed.2021.738425.

[16] H. Zhang *et al.*, "Deep Learning Model for the Automated Detection and Histopathological Prediction of Meningioma," *Neuroinformatics*, vol. 19, no. 3, pp. 393–402, Jul. 2021, doi: 10.1007/s12021-020-09492-6.

[17] S. C. Ng, "Principal component analysis to reduce dimension on the digital image," *Procedia Comput. Sci.*, vol. 111, pp. 113–119, 2017, doi: 10.1016/j.procs.2017.06.017.

[18] P. Suetens, *Fundamentals of medical imaging*, 2nd ed. Cambridge: Cambridge University Press, 2009.

[19] M. Gao, D. Qi, H. Mu, and J. Chen, "A Transfer Residual Neural Network Based on ResNet-34 for Detection of Wood Knot Defects," *Forests*, vol. 12, no. 2, p. 212, Feb. 2021, doi: 10.3390/f12020212.

[20] Padma Usha M, Kannan G, Ramamoorthy M, Sharmila M, Huzaifa Anjum G.A, and Hairunnisha M.S.H, "Multimodal Brain Image Fusion using Graph Intelligence Method," *Int. J. Res. Pharm. Sci.*, vol. 11, no. 2, pp. 2713–2724, Jun. 2020, doi: 10.26452/ijrps.v11i2.2293.

[21] J. Cheng *et al.*, "Enhanced Performance of Brain Tumor Classification via Tumor Region Augmentation and Partition," *PLOS ONE*, vol. 10, no. 10, p. e0140381, Oct. 2015, doi: 10.1371/journal.pone.0140381.

[22] W. Jun and Z. Liyuan, "Brain Tumor Classification Based on Attention Guided Deep Learning Model," *Int. J. Comput. Intell. Syst.*, vol. 15, no. 1, p. 35, Dec. 2022, doi: 10.1007/s44196-022-00090-9.

[23] M. Ramamoorthy, S. Qamar, R. Manikandan, N. Z. Jhanjhi, M. Masud, and M. A. AlZain, "Earlier Detection of Brain Tumor by Pre-Processing Based on Histogram Equalization with Neural Network," *Healthcare*, vol. 10, no. 7, p. 1218, Jun. 2022, doi: 10.3390/healthcare10071218.

[24] M. Kolla, R. K. Mishra, S. Zahoor ul Huq, Y. Vijayalata, M. V. Gopalachari, and K.-A.

Siddiquee, “CNN-Based Brain Tumor Detection Model Using Local Binary Pattern and Multilayered SVM Classifier,” *Comput. Intell. Neurosci.*, vol. 2022, pp. 1–9, Jun. 2022, doi: 10.1155/2022/9015778.

[25] M.Padma Usha, G.Kannan, and M.Ramamoorthy, “Multimodal Image Fusion with Segmentation for Detection of Brain Tumor Using Deep Learning Algorithm,” in *Application of Deep Learning Methods in Healthcare and Medical Science*, Apple Academic Press, pp. 165–176.

[26] S. Chitnis, R. Hosseini, and P. Xie, “Brain tumor classification based on neural architecture search,” *Sci. Rep.*, vol. 12, no. 1, p. 19206, Nov. 2022, doi: 10.1038/s41598-022-22172-6.

[27] M. Ahmed Hamza *et al.*, “Optimal and Efficient Deep Learning Model for Brain Tumor Magnetic Resonance Imaging Classification and Analysis,” *Appl. Sci.*, vol. 12, no. 15, p. 7953, Aug. 2022, doi: 10.3390/app12157953.

[28] Y.-L. Tai, S.-J. Huang, C.-C. Chen, and H. H.-S. Lu, “Computational Complexity Reduction of Neural Networks of Brain Tumor Image Segmentation by Introducing Fermi–Dirac Correction Functions,” *Entropy*, vol. 23, no. 2, p. 223, Feb. 2021, doi: 10.3390/e23020223.

Ms. M. Padmausha received a Master of Engineering in Communication Systems from Anna University, Chennai, India in the year 2008. She completed her undergraduate in B.Tech Electronics at Madras Institute of Technology, Chennai in the year 2005. Currently, she is working as an Assistant Professor (Senior Grade) in the Department of Electronics and Communication Engineering of B.S.Abdur Rahman Crescent Institute of Science and Technology Chennai, India. She has fourteen years of teaching experience. She currently works in the domain of Medical image processing and Artificial Intelligence

Dr.G Kannan received a Ph.D. degree from Anna University Chennai, India, an M.Tech in Embedded Systems from SASTRA University Thanjavur, and B.E Electronics and Instrumentation Engineering from Bharadhidasan University Tiruchirappalli in the year 2014, 2005 and 2000 respectively. At present, he is working as an Associate Professor in the Department of Electronics and Communication Engineering of B.S.Abdur Rahman Crescent Institute of Science and Technology Chennai, India. He has 15 years of teaching & research experience and his areas of research include Wireless Sensor Networks, System level power management in Embedded Systems, Real-Time Operating Systems, and Artificial Intelligence.

Mr. S. Sai Akshay is currently pursuing his B.Tech degree in the Electronics and Communications department at B.S. Abdur Rahman Institute of Science and Technology, Vandalur, Chennai. His areas of interest are Data Science, Machine Learning, and Image Processing.

Mr. Giri. S is currently pursuing his B.Tech degree in the Electronics and Communications department at B.S. Abdur Rahman Institute of Science and Technology, Vandalur, Chennai. His areas of interest are Image Processing, Automation, and Embedded Systems.

Mr. Shaik Muhammad Huzaifa is currently pursuing his B.Tech degree in the Electronics and Communications department at B.S. Abdur Rahman Institute of Science and Technology, Vandalur, Chennai. His areas of interest are Python Development and Data Science.